In situ transmission electron microscopy analysis of conductive filament during solid electrolyte resistance switching

Takashi Fujii,[1,a)] Masashi Arita,[1] Yasuo Takahashi,[1] and Ichiro Fujiwara[2]
[1]*Graduate School of Information Science and Technology, Hokkaido University, Sapporo 060-0814, Japan*
[2]*Semiconductor Technology Academic Research Center, 3-17-2 Shinyokohama, Kohoku-ku, Yokohama 222-0033, Japan*

(Received 7 February 2011; accepted 3 May 2011; published online 23 May 2011)

An *in situ* transmission electron microscopy (TEM) analysis of a solid electrolyte, Cu–GeS, during resistance switching is reported. Real-time observations of the filament formation and disappearance process were performed in the TEM instrument and the conductive-filament-formation model was confirmed experimentally. Narrow conductive filaments were formed corresponding to resistance switching from high- to low-resistance states. When the resistance changed to high-resistance state, the filament disappeared. It was also confirmed by use of selected area diffractometry and energy-dispersive x-ray spectroscopy that the conductive filament was made of nanocrystals composed mainly of Cu. © *2011 American Institute of Physics*. [doi:10.1063/1.3593494]

Solid electrolyte resistance random access memory (ReRAM) has great potential as nonvolatile memory.[1,2] It is scalable to a nanometer size because of its simple structure and its conduction paths at the nanometer scale.[3] Many previous studies reported resistance switching in solid electrolytes such as AgGeS,[4–7] CuGeS,[5] Cu_2S,[8] Ag_2S,[9,10] Ta_2O_5,[3,11] Cu-SiO_2,[12] and bilayer-types.[13,14] The mechanism of resistance switching is attributed to the formation and disappearance of the conductive filament in the solid electrolyte. When a bias voltage is applied, the ions generated at the anode are thought to migrate toward the cathode where they undergo reduction and become metal atoms.[8] Contrarily, an opposite bias voltage dissolves the metal composing filaments into the solid electrolyte.[11] Therefore, an analysis of the conductive filament must provide important information for understanding this switching mechanism. Recently, conductive filament, which is formed in not only cation-type but also in anion-type electrolytes, was observed by scanning electron microscopy (SEM).[5,15,16] However, no detailed experimental results to confirm the existence of the filament during the switching process have been reported. Therefore, *in situ* transmission electron microscopy (TEM) with simultaneous electrical measurements has attracted a great deal of attention.[10,17–21]

In this letter, we use this *in situ* TEM method to reveal the switching mechanism of a solid electrolyte. Real-time observations of the filament formation and disappearance process were performed with the TEM instrument. We also clarified the structure and composition of the filament by the use of selected area diffractometry (SAD) and energy-dispersive x-ray spectroscopy (EDX).

For the *in situ* TEM experiments,[21] commercially available Pt–Ir tips for scanning tunneling microscopy were further sharpened by ion milling. One Pt–Ir tip was used as the substrate and the other was used as a counter electrode. Cu–GeS thin films were deposited at room temperature by rf sputtering on Pt–Ir substrate. Since the substrate and the counter electrode of Pt–Ir were different in shape, the structure of Pt–Ir/Cu–GeS/Pt–Ir was asymmetric. The atomic composition of the sample layer was analyzed by means of EDX. The proportion of Cu:Ge:S was 4:4:2. The film thickness was between 8 and 60 nm, and no remarkable difference depending on thickness was recognized. The system was composed of a custom-made TEM holder with a PC-controlled operating system.[21–23] The TEM instrument used mainly was a JEM-2010 microscope (200 kV, C_s=0.5 mm), having a vacuum of about 10^{-5} Pa. The conduction properties were measured between the Pt–Ir counter electrode and the Cu–GeS/Pt–Ir. The best location of measuring I-V characteristics was selected in the fixed Cu–GeS/Pt–Ir sample by moving the Pt–Ir counter electrode. The TEM images were recorded using a CCD video camera.

Prior to the current-to-voltage (I-V) measurement, TEM observation of Cu–GeS were carried out. It was confirmed that the Cu–GeS layer was smoothly deposited on the Pt–Ir tips and that Cu–GeS was in an amorphous phase including the nanocrystals. This was also recognized in SAD patterns obtained from a wide area. The structure changes were not observed even during high resolution TEM observations (beam current density at the sample; about 170 fA/nm^2). The *in situ* TEM experiments described below were performed with lower beam current. Thus, the influence of the electron beam should be negligible.

The I-V curve measured in the TEM instrument is shown in Fig. 1, in which the voltage is the potential of the substrate relative to the counter electrode. The voltage was swept from 0 to 7 V, from 7 to −2 V, and back to 0 V. The I-V curve shows a typical resistance switching characteristics with hysteresis. Figure 2 shows a set of TEM images corresponding to Fig. 1. The resistance changed from high resistance states (HRS) to low resistance states (LRS) occurred at around 1 V. Corresponding to this change, a small deposit appeared as shown in Fig. 2(b).

The growth of the deposit was almost stopped after current increase [Figs. 2(c)–2(g)] even though the current level and the resistance change up and down according to the voltage scan. In this process, even if the size of the deposit is almost constant, some changes were occurred around the deposit. It was confirmed that the diffraction spots of the SAD twinkled continuously during the voltage scan. The current crossing at about 2 V and sudden current increase at about

a)Electronic mail: t-fujii@ist.hokudai.ac.jp.

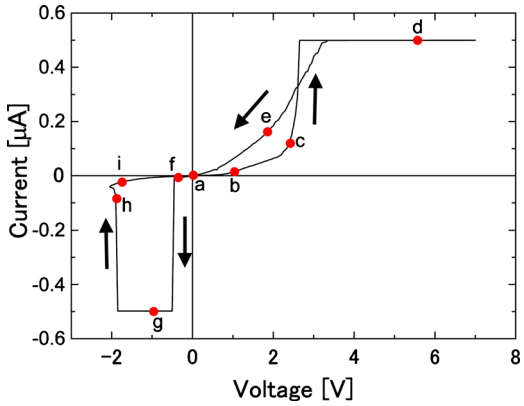

FIG. 1. (Color online) I-V characteristics measured with a TEM instrument. The voltage swept from 0 to 7 V, 7 to −2 V, and back to 0 V with a current limit of 0.5 μA.

−0.5 V may be caused by over accumulation of Cu to the needle side in the Cu–GeS film. The accumulation was released by applying slight negative voltage of −0.5 V.

The deposit suddenly shrank [Fig. 2(h)] at about −2 V, and completely disappeared [Fig. 2(i)]. The sample resistance turned back to HRS. The size of the deposit and the current value corresponded to each other. From these results shown in Figs. 1 and 2, it was concluded that the deposit observed in Fig. 2 constitutes the conducting path.

As shown in Fig. 3, the crystal structure of the deposit was studied by observing real-time SAD patterns during voltage application, which were from the wide area where the Pt–Ir substrate and the counter electrode were situated.

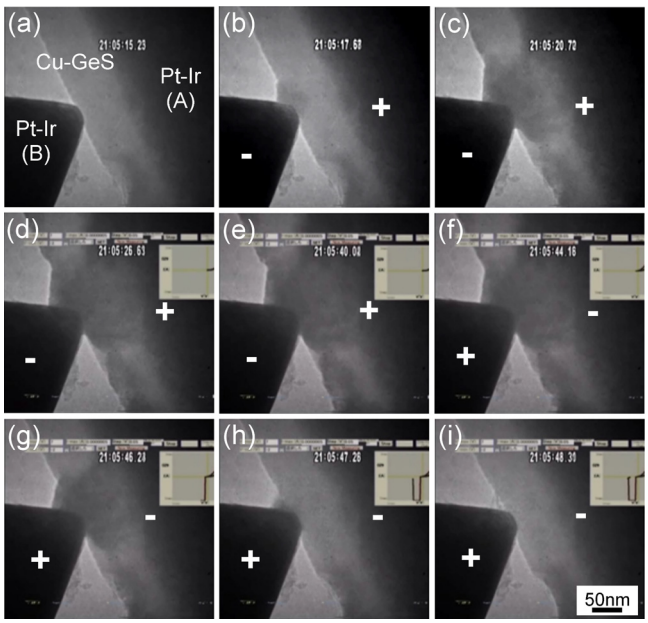

FIG. 2. (Color online) Series of TEM images during voltage application. The symbols "+" and "−" indicate the polarity of voltage. Each figure corresponds to points **a** to **j** shown in Fig. 1, respectively. (a) Cu–GeS (A) contacted by the Pt–Ir (B). [(b) and (c)] Deposit appeared and grew in the Cu–GeS with the application of positive voltage. The resistance gradually decreased. [(d) and (e)] The resistance rapidly decreased when the deposit connected between two Pt–Ir tips. The deposit size was saturated. [(f) and (g)] No change was confirmed in the deposit. The resistance maintained LRSs during voltage sweeping. (h) The deposit was suddenly shrunk with the increasing negative voltage. Disconnected deposit caused to high resistance. (i) Complete disappearance of the deposit.

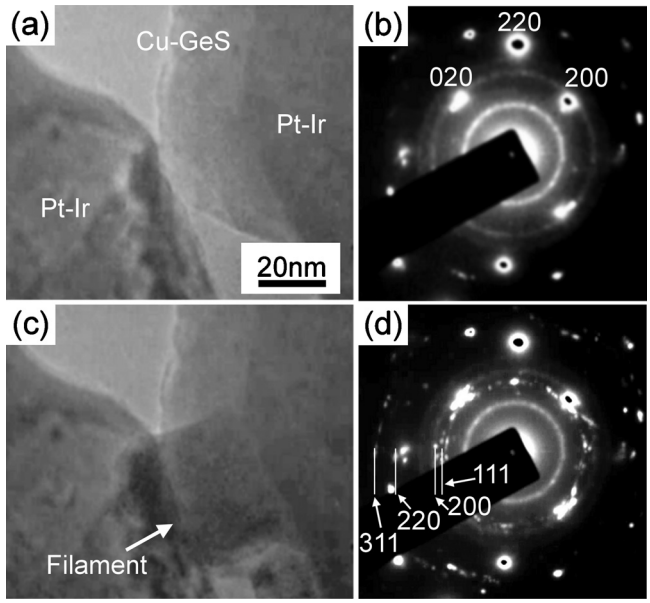

FIG. 3. (a) TEM image and (b) SAD pattern before voltage application. Clear spots caused by Pt–Ir and weak Debye-ring patterns were observed. The latter diffraction, which did not change during the resistance switching operation, may come from the Ge nanocrystals. The indices are those of Pt–Ir. (c) TEM image and (d) SAD pattern during voltage application of 1 V. The filamentlike deposit and the appearance of fine and sharp diffraction spots forming Debye-rings were recognized. They are thought to be from Cu nanocrystals, four of which corresponded with reflection indices.

To minimize the influence of regions other than those near the deposit, a corner of the Cu–GeS layer was selected to be investigated [Fig. 3(a)]. The SAD pattern before applying voltage [Fig. 3(b)] was composed of a faint background and Debye rings. This corresponds to characteristics found in the TEM image described above, i.e., amorphous with nanocrystals. The clear spots in this pattern were caused by Pt–Ir. Using these spots as references, it was concluded that the faint rings corresponded to the 111, 220, and 311 reflections of the Ge. By applying 1 V to the substrate, a deposit appeared as seen in Fig. 2. Its width was about 40 nm [Fig. 3(c)]. At this voltage, sharp spots appeared in the SAD pattern in addition to Fig. 3(b). They twinkled like stars in the night sky. This SAD pattern indicates that well crystallized nanocrystals were generated by the voltage application, and their orientation frequently changed during the growth of the deposit. To analyze this process in detail, 1152 frames of video images totaling 35 s were superposed [Fig. 3(d)]. Relatively sharp spots that formed rings were recognized. These rings have d-values similar to those of the 111, 200, 220, and 311 reflections of the Cu. These results clearly show that main material forming the deposit was the nanocrystals of Cu or diluted Cu alloy with either Ge and/or S.

The EDX spectra of the area before and after positive voltage (1 V) application are shown in Fig. 4. The sample was the 8-nm-thick Cu–GeS where the deposit appeared. The beam size for the EDX measurements was about 10 nm. Therefore, in the obtained spectra [Figs. 4(a) and 4(b)], the Pt peaks of the electrodes were superposed. The intensity of the Cu peak greatly increased during the voltage application. By assuming the thin foil approximation, the estimated composition of the deposit for Cu:Ge:S was 7:2:1 [Fig. 4(b)], while it was 4:4:2 without the deposit [Fig. 4(a)]. Although this approximation gives rough estimation to discuss in de-

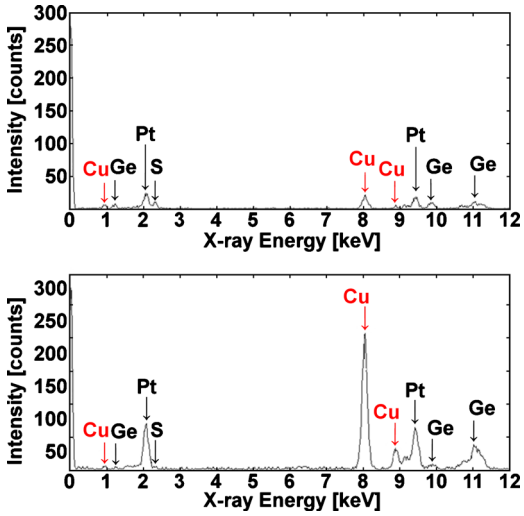

FIG. 4. (Color online) (a) EDX spectrum before voltage application. The relative concentration was estimated as Cu:Ge:S=4:4:2. (b) EDX spectrum during 1 V application. The Cu peak was strong from the deposit. The relative concentration of the deposit was estimated as Cu:Ge:S=7:2:1.

tail, it can be summarized by saying that the deposit was an agglomeration of crystals with a relatively large amount of Cu.

The conductive filament is assumed to be formed in the observed deposit. During filament formation, Cu ions dissolving in the GeS may move to the cathode and become metal atoms. The polarity dependence in this work may be attributed to the asymmetry of the electric field caused by the shape difference between the substrate and counter electrode as clearly seen in Fig. 2. We investigated various thicknesses of the Cu–GeS layers, and similar phenomena were observed in all cases.

In summary, we confirmed the resistance switching of Cu–GeS films by *in situ* TEM and confirmed the conductive-filament-formation model experimentally by means of real time observation. The formation and disappearance of the conductive filament were clearly observed in the switching operation. From SAD and EDX results, it was determined that the conductive filament consisted of nanocrystals composed mainly of Cu.

We thank Mr. S. Yasuda (Sony Corporation) for his collaboration in device fabrication, and Dr. M. Moniwa, Dr. T. Yamaguchi, and Dr. M. Yoshimaru (Semiconductor Technology Academic Research Center) for their fruitful discussion. The TEM-EDX analyses were performed at CAREM, Hokkaido University with the kind support of Professor N. Sakaguchi, to whom we are grateful.

[1]R. Waser and M. Aono, Nature Mater. **6**, 833 (2007).
[2]R. Waser, R. Dittmann, G. Staikov, and K. Szot, Adv. Mater. (Weinheim, Ger.) **21**, 2632 (2009).
[3]Y. Tsuji, T. Sakamoto, N. Banno, H. Hada, and M. Aono, Appl. Phys. Lett. **96**, 023504 (2010).
[4]M. N. Kozicki, M. Park, and M. Mitkova, IEEE Trans. Nanotechnol. **4**, 331 (2005).
[5]M. N. Kozicki, M. Balakrishnan, C. Gopalan, C. Ratnakumar, and M. Mitkova, *Proceedings of IEEE Non-Volatile Memory Technology Symposium* (IEEE, New York, 2005), Vol. 83.
[6]M. N. Kozicki, C. Ratnakumar, and M. Mitkova, *Proceedings of IEEE Non-Volatile Memory Technology Symposium* (IEEE, New York, 2006), Vol. 111.
[7]D. Kamalanathan, U. Russo, D. Ielmini, and M. N. Kozicki, IEEE Electron Device Lett. **30**, 553 (2009).
[8]T. Sakamoto, H. Sunamura, H. Kawaura, T. Hasegawa, T. Nakayama, and M. Aono, Appl. Phys. Lett. **82**, 3032 (2003).
[9]K. Terabe, T. Hasegawa, T. Nakayama, and M. Aono, Nature (London) **433**, 47 (2005).
[10]Z. Xu, Y. Bando, W. Wang, X. Bai, and D. Golberg, ACS Nano **4**, 2515 (2010).
[11]T. Sakamoto, K. Lister, N. Banno, T. Hasegawa, K. Terabe, and M. Aono, Appl. Phys. Lett. **91**, 092110 (2007).
[12]C. Schindler, G. Staikov, and R. Waiser, Appl. Phys. Lett. **94**, 072109 (2009).
[13]M. Tada T. Sakamoto N. Banno, M. Aono, H. Hada, and N. Kasai, IEEE Trans. Electron Devices **57**, 1987 (2010).
[14]K. Aratani, K. Ohba, T. Mizuguchi, S. Yasuda, T. Shiimoto, T. Tsushima, T. Sone, K. Endo, A. Kouchiyama, S. Sasaki, A. Maesaka, N. Yamada, and H. Narisawa, Tech. Dig. Int. Electron Devices Meet. **2007**, 783.
[15]K. Fujiwara, T. Nemoto, M. J. Rozenberg, Y. Nakamura, and H. Takagi, Jpn. J. Appl. Phys. **47**, 6266 (2008).
[16]R. Yasuhara, K. Fujiwara, K. Horiba, H. Kumigashira, M. Kotsugi, M. Oshima, and H. Takagi, Appl. Phys. Lett. **95**, 012110 (2009).
[17]Ch. Jooss, J. Hoffmann, J. Fladerer, M. Ehrhardt, T. Beetz, L. Wu, and Y. Zhu, Phys. Rev. B **77**, 132409 (2008).
[18]D. Cha, S. J. Ahn, S.Y. Park, H. Horii, D. H. Kim, Y. K. Kim, S. O. Park, U. I. Jung, M. J. Kim, and J. Kim, Dig. Tech. Pap. - Symp. VLSI Technol. **2009**, 204.
[19]T. Fujii, H. Kaji, H. Kondo, K. Hamada, M. Arita, and Y. Takahashi, IOP Conf. Ser.: Mater. Sci. Eng. **8**, 012033 (2010).
[20]D.-H. Kwon, K. M. Kim, J. H. Jamg, M. Jeon, M. H. Lee, G. H. Kim, X.-S. Li, G.-S. Park, B. Lee, S. Han, M. Kim, and C. S. Hwang, Nat. Nanotechnol. **5**, 148 (2010).
[21]T. Fujii, M. Arita, K. Hamada, H. Kondo, H. Kaji, Y. Takahashi, M. Moniwa, I. Fujiwara, T. Yamaguchi, M. Aoki, Y. Maeno, T. Kobayashi, and M. Yoshimaru, J. Appl. Phys. **109**, 053702 (2011).
[22]R. Hirose, M. Arita, K. Hamada, and Y. Takahashi, Jpn. J. Appl. Phys., Part 2 **44**, L790 (2005).
[23]M. Arita, Y. Okubo, K. Hamada, and Y. Takahashi, Superlattices Microstruct. **44**, 633 (2008).